energies

MDPI

Article

Supercapacitor Storage Sizing Analysis for a Series Hybrid Vehicle

Massimiliano Passalacqua [1], Mauro Carpita [2], Serge Gavin [2], Mario Marchesoni [1,*], Matteo Repetto [3], Luis Vaccaro [1] and Sébastien Wasterlain [2]

1 Department of Electrical, Electronic, Tlc Engineering and Naval Architecture (DITEN), University of Genoa, via all'Opera Pia 11a, 16145 Genova, Italy; massimiliano.passalacqua@edu.unige.it (M.P.); luis.vaccaro@unige.it (L.V.)

2 Institute of Energy and Electrical Systems (IESE), University of Applied Sciences of Western Switzerland, route de Cheseaux 1, CH 1400 Yverdon-les-Bains, Switzerland; mauro.carpita@heig-vd.ch (M.C.); serge.gavin@heig-vd.ch (S.G.); sebastien.wasterlain@heig-vd.ch (S.W.)

3 Department of Mechanical, Energy, Management and Transportation Engineering (DIME), University of Genova, via all'Opera Pia 15, 16145 Genova, Italy; salabi@unige.it

* Correspondence: marchesoni@unige.it

Received: 9 April 2019; Accepted: 5 May 2019; Published: 9 May 2019

Abstract: The increasing interest in Hybrid Electric Vehicles led to the study of new powertrain structures. In particular, it was demonstrated in the technical literature how series architecture can be more efficient, compared to parallel one, if supercapacitors are used as storage system. Since supercapacitors are characterized by high efficiency and high power density, but have low specific energy, storage sizing is a critical point with this technology. In this study, a detailed analysis on the effect of supercapacitor storage sizing on series architecture was carried out. In particular, in series architecture, supercapacitor storage sizing influences both engine number of starts and the energy that can be stored during regenerative braking. The first aspect affects the comfort, whereas the second aspect directly influences powertrain efficiency. Vehicle model and Energy Management System were studied and simulations were carried out for different storage energy, in order to define the optimal sizing.

Keywords: Hybrid Electric Vehicle (HEV); series architecture; supercapacitor; Energy Management System (EMS); storage sizing; energy efficiency

1. Introduction

Hybrid Electric Vehicles (HEVs) have experienced a great interest in the last decades thanks to increasing attention both in carbon emission and local pollutant reduction. On the one hand, HEVs, by increasing overall powertrain efficiency, can reduce CO_2 emissions; on the other hand, allowing electric traction in urban missions and smoothing Internal Combustion Engine (ICE) accelerations, they can reduce local pollutant emissions. In the technical literature, different hybrid topologies and many Energy Management Systems (EMS) were proposed [1,2] nevertheless hybrid architectures can be mainly divided in two categories: parallel and series hybrid vehicles. Regarding parallel architecture, this structure is mainly used on medium size cars and can be realized either with one electrical machine [3–7], two electrical machines and a planetary gearbox (also known as power split or series/parallel hybrid) [8–14] can be realized with a compound structured permanent-magnet motor [15]. As far as series architecture is concerned, this topology was mainly designed, until now, for urban bus applications [16–18]. However, innovations and developments in storage systems and power electronics may change this paradigm. Analyzing storage system innovations, the supercapacitor

significantly increased their performance in terms of energy density [19,20], so that their use become possible with a proper sizing; indeed many studies focused on the combined use of supercapacitors and batteries as storage system in hybrid vehicle applications [21–25]. In addition to that, the availability of low-loss power electronics devices, such as Silicon Carbide (SiC) metal-oxide-semiconductor field-effect transistor (MOSFET) [26,27], allows to design high efficiency power converter. Storage systems and power converters efficiency highly influence series architecture fuel consumption. As a matter of fact, in [28], it was shown how parallel architecture fuel consumption is slightly affected by storage and converters efficiency; indeed, these components are mainly used to recover (and reuse) backward energy deriving from regenerative braking. On the contrary, in the series architecture, all the energy provided by the ICE incurs in a double conversion (i.e., from mechanical to electrical and from electrical to mechanical) and the instantaneous difference between the power provided by the ICE and the power required by the electric motor is balanced by the storage system. As a consequence, energy flows, both in power converters and storage system, are significantly higher compared to parallel architecture and the efficiency of these components highly influences powertrain fuel consumption.

Authors in [29] proposed a series architecture for medium size cars based on supercapacitor storage and they showed the benefit of this solution in terms of fuel consumption in comparison to parallel architecture. Although all the energy provided by the ICE is affected by the generator, generator inverter, motor inverter and motor losses, series architecture allows the ICE to work in optimal working condition (i.e., high efficiency) and, as a result, the overall powertrain efficiency is higher. In particular, they proposed an EMS to properly use the supercapacitor storage, which aims both at increasing the system efficiency and the comfort (i.e., reducing ICE number of starts and ICE provided power at low vehicle speed). That study was carried out hypothesizing a 465 Wh storage system.

However, a detailed analysis on storage optimal sizing has not yet been carried out and remains a topic of great interest. As a matter of fact, storage sizing is a current issue and was investigated in the technical literature for electric vehicle using a combined battery-supercapacitor storage [30] and for fuel cell hybrid vehicle, again using a combined battery-supercapacitor storage [31]. Nevertheless, since series hybrid architecture on a medium size car using only supercapacitor storage was proposed for the first time in [29], a study on storage sizing in this application is still missing. In this paper, the effect of storage sizing on hybrid powertrain will be shown. In particular, the impact on both powertrain efficiency and ICE management will be investigated. The study will be performed on a significant number of road missions, in order to consider a wide range of possible working conditions. Standard cycles will be taken into account: Highway Fuel Economy Test (HWFET), Urban Dynamometer Driving Schedule (UDDS) and the Supplemental Federal Test Procedures (SFTP or US06) [32]; nevertheless, being these type approvals in plane missions, backward energy is limited and therefore they are not critical for storage sizing. For this reason, a large number of experimentally measured missions will be considered, including also mountain roads with a great change in altitude.

On balance, the main innovative contributions of this research can be pinpointed as follows: (1) analysis of supercapacitor storage sizing influences on ICE number of starts in a series hybrid vehicle, (2) supercapacitor storage sizing influences on fuel consumption, evaluated both with a spark-ignition engine and a diesel engine, and (3) feasibility of a series hybrid vehicle using only supercapacitor as a storage system.

The paper is structured as follows: in Section 2 series architecture is presented and EMS is described, focusing, in particular, on storage system parameters. Storage zones analysis and sizing optimization are shown in Section 3, whereas road missions are shown in Section 4. Simulation results are reported in Section 5. Finally, conclusions are pointed out in Section 6.

2. Series Architecture and Energy Management System (EMS)

Series architecture structure is depicted in Figure 1, where contour maps show powertrain components efficiency. The aim of the study was the analysis of storage sizing on powertrain efficiency,

a quasi-stationary model was created in MATLAB/Simulink environment [29,33]. As a matter of fact, dynamic behavior of the different components is not relevant to energy evaluation. Each component was modeled, taking into account its efficiency contour map, as reported in Figure 1. Machine efficiency is given as a function of per-unit torque and per-unit speed, according to what was presented in [33]; in this way, the same contour map can be used also for different machine sizing. The same approach was used to model inverter losses, which are given in per-unit (i.e., referred to inverter nominal power). DC/DC converter efficiency is given as a function of storage voltage and current, supposing a 650 V DC-link. Vehicle longitudinal dynamic parameters (i.e., vehicle mass, rolling coefficient, aerodynamic drag coefficient and front section) are also reported in Figure 1. Differential gear efficiency is considered as a constant parameter. Powertrain fuel consumption is evaluated both using a spark ignition engine and a diesel engine. The aim of the study is to properly size the supercapacitor storage (red circle in Figure 1).

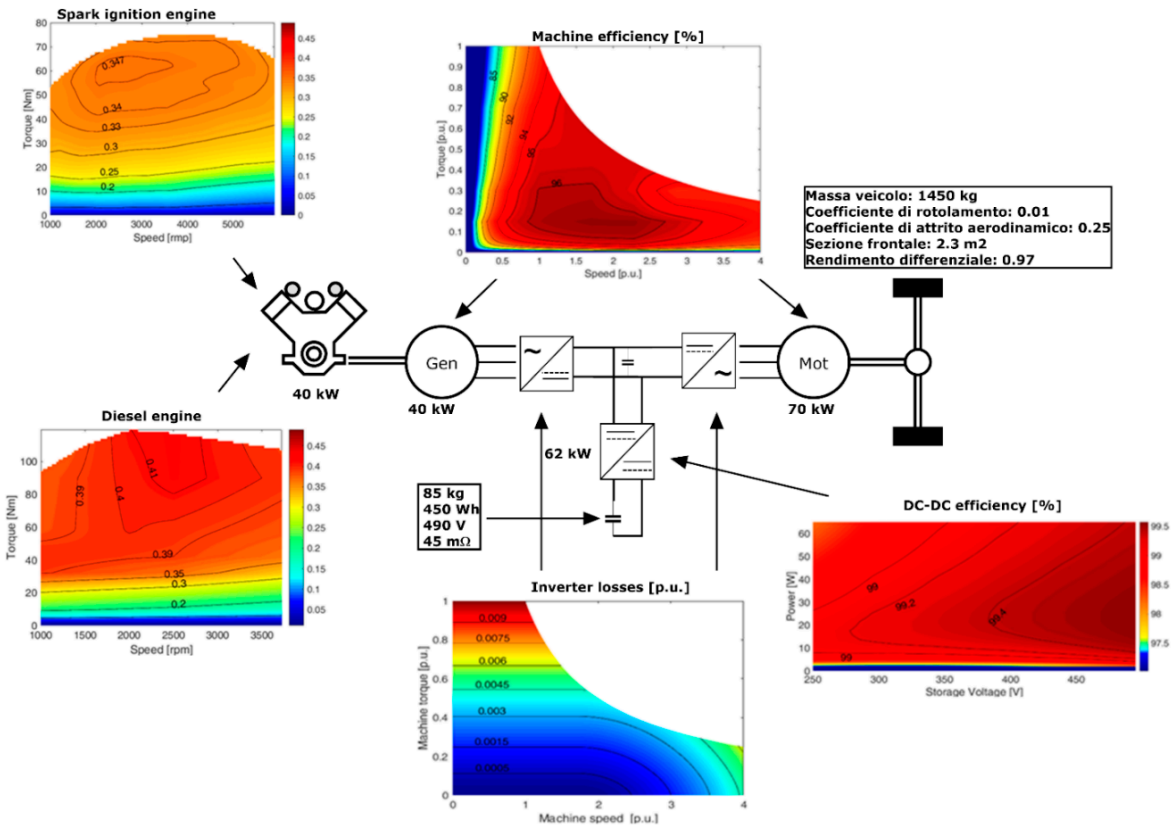

Figure 1. Series architecture structure. Contour maps show components efficiency.

Supercapacitor main features are reported in Table 1 both for Electrostatic Double-Layer capacitors (EDLCs) [19] and Lithium supercapacitors [20]. Fuel consumption evaluation was carried out considering EDLC supercapacitor; nevertheless, since lithium supercapacitor efficiency is quite close to EDLC, the resulting trend can be considered correct.

Table 1. Supercapacitor (SC) features.

Feature	EDLC SC	Lithium SC
Cell energy density	7–8 Wh/kg	10–13 Wh/kg
Package energy density [1]	3.5–4 Wh/kg	5–7 Wh/kg
Cell maximum voltage	2.8–3 V	3.8 V
Round trip efficiency at 120 s [2]	96–98%	94–97%

[1] Energy density considering cells, package, connections between cells and cell management system weight. [2] Charge—discharge efficiency with a DC current that can charge (or discharge) the storage in 60 s. EDLC: Electrostatic Double-Layer capacitors.

According to the EMS proposed in [29], one can define four storage voltage working zones (three allowed zones and a forbidden one):

- Braking zone (UVL < V < V_{max}):
- Normal zone (LVL < V < UVL)
- Low speed zone (V_{limit} < V < LVL)
- Forbidden zone (V < V_{limit})

where UVL (Upper Voltage Limit) and LVL (Lower Voltage Limit) are two settable parameters, V_{max} is the storage rated voltage and V_{limit} is the storage lower allowed voltage (which can be either a storage or a converter constraint). In this study, V_{limit} is set to 0.5 V_{max}, whereas LVL and UVL definition is one of the objective of the research. V_{ref} is another settable parameter, the aim of which is explained in detail in page 5.

The braking zone is devoted to regenerative brakings, whereas the low speed zone is devoted to electrical traction at low vehicle speed. In addition to storage zone definition, and consequently LVL and UVL definition, it is necessary to identify also two vehicle speed thresholds: a Lower Speed Limit (LSL) and an Upper Speed Limit (USL).

Once these parameters are defined, one can illustrate the Engine Ignition Management System (EIMS), which regulates ICE starts and stops. The EIMS decision depends on storage state of charge, vehicle speed and ICE condition (i.e., if engine is already on or not), as shown in Figure 2.

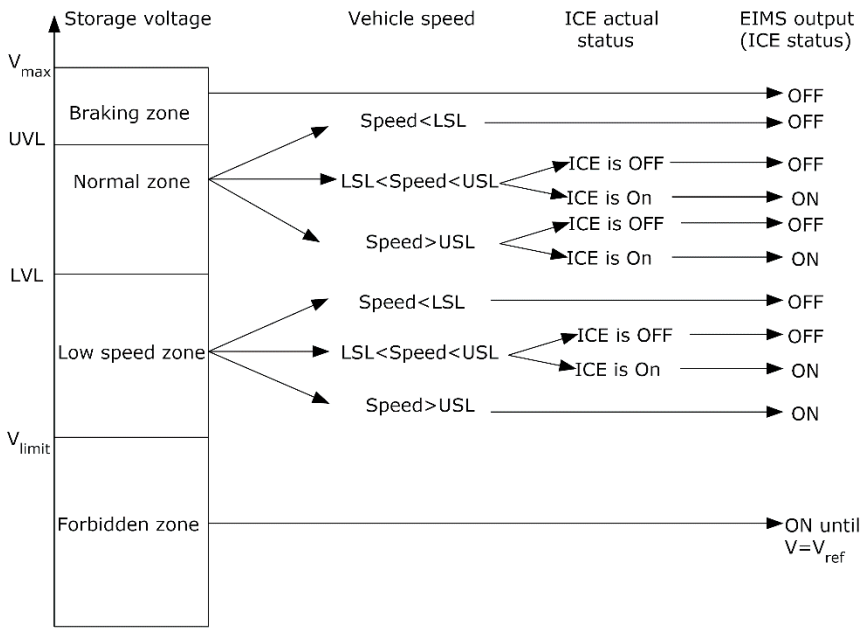

Figure 2. Engine Ignition Management System (EIMS).

The EIMS decides whether the ICE has to be turned on, turned off or it has to remain in the current condition; nevertheless, once the EIMS has decide the ICE should be turned on, the proposed Engine Power Management System (EPMS) [29] controls the ICE output power, as shown in Figure 3.

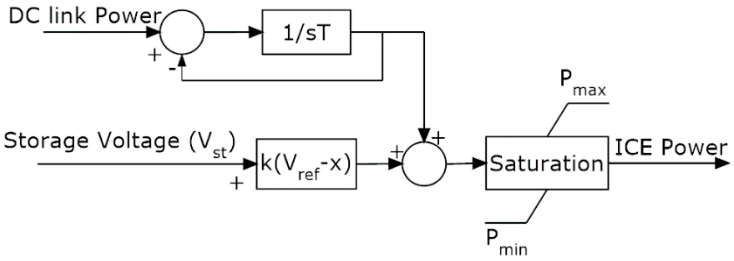

Figure 3. Engine Power Management System (EPMS).

The output power of the EPMS is given by the filtered DC-link required power and a contribution which depends on storage voltage (i.e., storage state of charge). This structure avoids high engine speed (i.e., high engine power) when the required power is low. As a matter of fact, high engine speed when the required power is low (e.g., when vehicle speed is low) is an uncomfortable condition. The power required at the DC-link is filtered in order to smooth acceleration and therefore reduce pollutant emissions [34,35].

The EPMS output is saturated between P_{max} (i.e., ICE rated power), and P_{min}, which is the ICE output power until which engine efficiency is still high; from ICE contour maps in Figure 1 indeed, it is possible to notice that efficiency worsens significantly in low power working conditions. When the DC-link required power is higher than P_{min} (e.g., in highway missions) the EPMS keeps storage voltage around V_{ref}. On the contrary, when the required power is lower than P_{min}, the ICE charges the storage system until UVL and then turns off until storage voltage reaches LVL. For this reason, if speed is higher than USL and the vehicle is not involved in long braking, storage voltage is always in the normal zone. The aim of the low speed zone definition is to keep the ICE off when vehicle starts and until it reaches USL. It is necessary to define both USL and LSL in order to reduce ICE number of starts when vehicle speed keeps around USL (or equally around LSL) for a long time.

The parameter T was set to 10 s, its optimization depends on ICE dynamic behavior and it is not considered in this study. Analogously, V_{ref} optimization depends on road mission profile (high values for highway missions, low values for long downhill road missions) and it can be set either manually by the driver or in a predictive way if the mission is known; in this study, it was set in the middle of UVL and LVL for all the missions. One has to note that V_{ref} has to be inside the normal zone. Parameter k was set to 0.06 kW/V (been V_{max} 500 V in all storage configurations). LSL and USL were set to 15 km/h and 30 km/h, respectively, whereas LVL and UVL optimization is one of the aims of this study, as shown in the next section. P_{min} was set to 6.6 kW for spark-ignition engine (power which corresponds to 34% efficiency, with maximum efficiency being 34.7%) and to 4.7 kW for diesel engine (power which corresponds to 39.5% efficiency, maximum efficiency being 41.5%). P_{max} was 40 kW for both spark-ignition and diesel engine.

3. Storage Zones Analysis and Sizing Optimization

The aim of the study is to analyze the influence of storage sizing on powertrain efficiency and on ICE number of starts (which affects comfort). Even if the sizing optimization of each of the three zones (the forbidden zone is not optimizable) is not independent from each other, the sizing of each zone has a precise consequence on powertrain performance:

- Braking Zone (BZ): if the braking zone is too small, there is a small quantity of energy available for regenerative braking. This influences powertrain efficiency, especially in missions characterized by long downhill roads. As a matter of fact, when the storage system reaches V_{max} the extra backward energy has to be dissipated on mechanical brakes.

- Normal Zone (NZ): if this zone is too small, the storage system charges and discharges quickly; as a consequence, ICE number of starts increases significantly.
- Low Speed Zone (LSZ): the aim of this zone is to avoid engine use at low speed. Indeed, one of hybrid vehicle aims is to guarantee electric traction at low speed. If the low speed zone is limited, ICE starts when vehicle speed is low (i.e., below USL) may occur frequently.

Although it is possible to identify a precise effect on powertrain management for each zone sizing, they still depend on each other. As an example, if the braking zone is limited but the energy associated to normal zone is high, there will be, on average, enough to store backward energy in the normal zone. Indeed, if no predictive control on the road mission is implemented, the braking phase can occur with the same probability in each point of the normal zone. Analogously, if the energy associated to the low speed zone is limited, but, again, the normal zone is large, ICE starts at low speed are infrequent. Nevertheless, low speed zone and braking zone sizing do not influence each other. Moreover, even if normal zone sizing influences the average storable energy during regenerative braking, braking zone sizing does not significantly influence the ICE number of starts; indeed, if storage voltage is in the braking zone, ICE is turned off until LVL is reached. In the same way, normal zone sizing influence low speed zone sizing, but low speed zone sizing do not significantly influences ICE number of starts when vehicle speed is above USL, which are only related to normal zone sizing.

The above considerations on zone sizing influences are summarized in the flowchart shown in Figure 4.

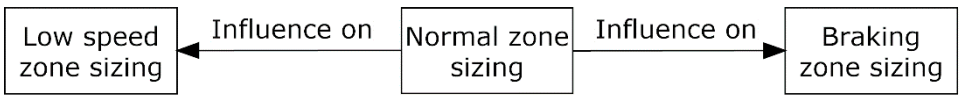

Figure 4. Zone sizing influences.

Taking into account the influences of Figure 4, the storage sizing analysis will be carried out as follows. Starting with an a priori defined sizing on low speed and braking zones, normal zone sizing influence on ICE number of starts will be analyzed. The analysis will be carried out on all the road missions considered in this study. Once a proper sizing has been defined, which will be a compromise between ICE number of starts and zone sizing, low speed zone and braking zone sizing will be investigated, the definition of which is almost independent from other zones once normal zone sizing has been established.

4. Road Missions

At first, standard cycles were considered: US06, UDDS and HWFET [32]. As can be noticed from Table 2, where road mission parameters are reported, these type approvals do not consider altitude variations; therefore, they are not critical for the supercapacitor storage, since there is no potential energy to recover during downhill roads.

Table 2. Road mission features.

Missions	Average Speed [km/h]	Maximum Speed [km/h]	Length [km]	Time [Minutes]	Change of Altitude [m]
US06	78	130	13	10	-
UDDS	31	90	12	23	-
HWFET	78	90	16.5	13	-
Urban	24	57	11.4	25	-
Fast-urban	27	68	22	52	62
Extra-urban 1	45	80	36	50	300
Mountain mission 1	48	85	24	30	500
Extra-urban 2	62	96	57	55	190
Mountain mission 2	51	90	60	70	710
Highway + mountain	87	125	480	330	1700

For this reason, experimentally measured missions were considered. Mission were measured with high precision GPS and barometric altimeter, with a 1 s sampling period. These road profiles were acquired in the north-west area of Italy (Liguria, Piemonte, Lombardia and Valle d'Aosta regions). The measured missions are:

- Urban: 11 km inside Aosta (Italy) town center.
- Fast-urban: from University of Genova, Albaro district (Genoa, Italy) to Bogliasco (Genoa, Italy) and return.
- Extra-urban 1: from University of Genova, Albaro district (Genoa, Italy) to Lavagna (Genoa, Italy) via Bargagli (Genoa, Italy).
- Mountain mission 1: Champorcher valley (Aosta, Italy) and return.
- Extra-urban 2: from Boves (Cuneo, Italy) to Mondovì (Cuneo, Italy).
- Mountain mission 2: from Boves (Cuneo, Italy) to Limonetto (Cuneo, Italy) and return.
- Highway + Mountain: from Milan (Italy) to Pont (Valsavaranche, Aosta, Italy) and return.

Road mission main features are summarized in Table 2, whereas speed and altitude profiles are shown in Figure 5 (Urban), Figures 6 and 7 (Fast-urban), Figures 8 and 9 (Extra-urban 1), Figures 10 and 11 (Mountain mission 1), Figures 12 and 13 (Extra-urban 2), Figures 14 and 15 (Mountain mission 2), Figures 16 and 17 (Highway + mountain mission). Since altitude change is negligible in urban mission, only speed profile is shown. Please note that, conventionally, initial altitude is set to zero in all missions; therefore, altitude has to be intended as the positive altitude difference during the mission and not as the absolute altitude value.

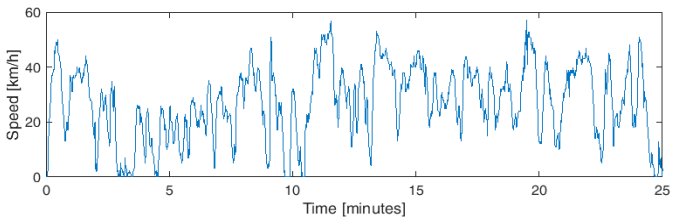

Figure 5. Urban.

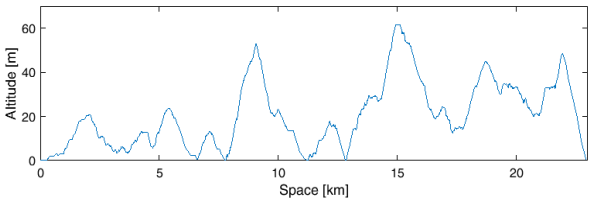

Figure 6. Fast-urban altitude profile.

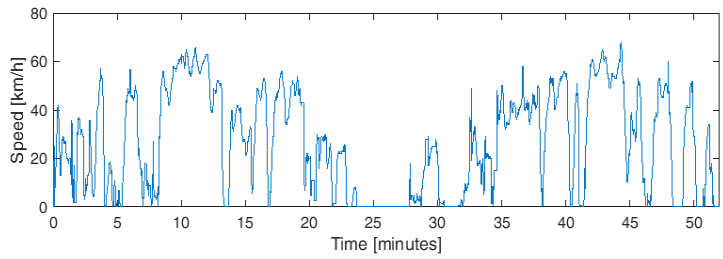

Figure 7. Fast-urban speed profile.

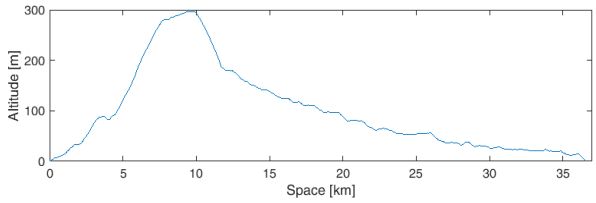

Figure 8. Extra-urban 1 altitude profile.

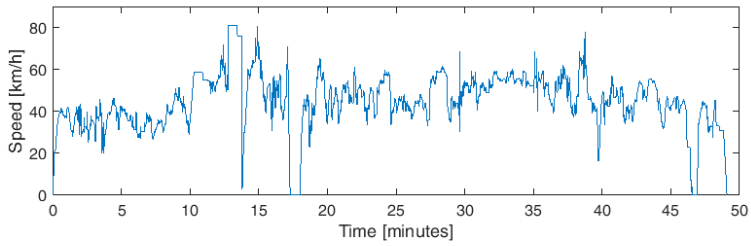

Figure 9. Extra-urban 1 speed profile.

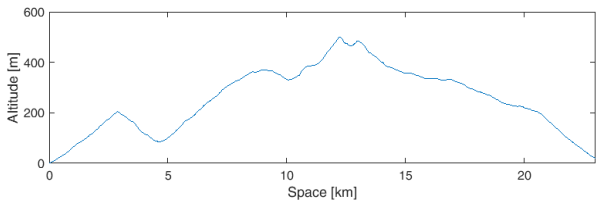

Figure 10. Mountain mission 1 altitude profile.

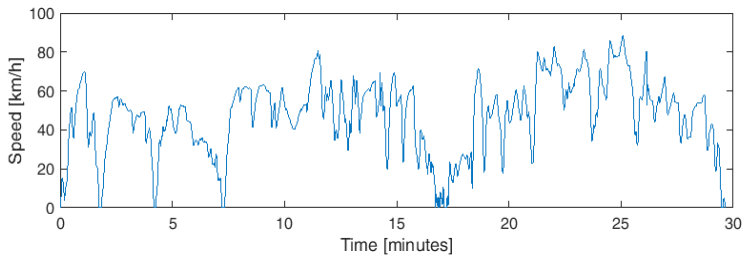

Figure 11. Mountain mission 1 speed profile.

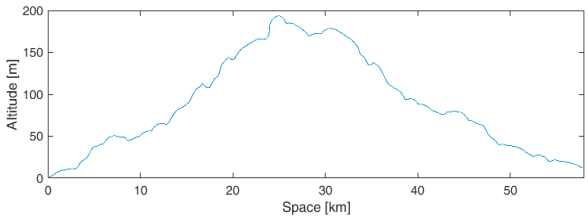

Figure 12. Extra-Urban 2 altitude profile.

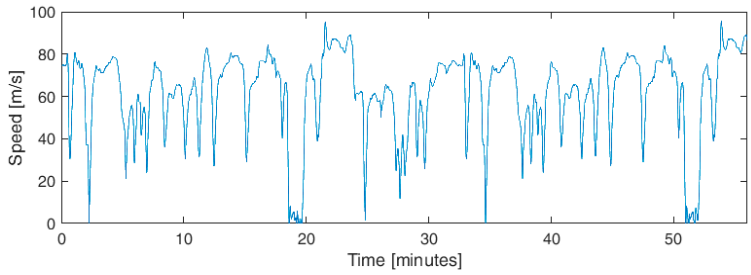

Figure 13. Extra-Urban 2 speed profile.

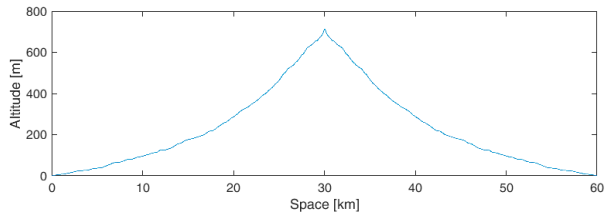

Figure 14. Mountain mission 2 altitude profile.

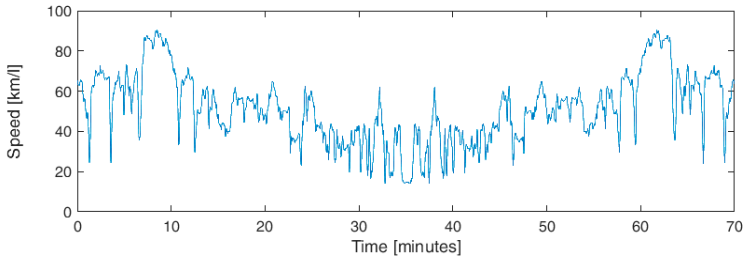

Figure 15. Mountain mission 2 speed profile.

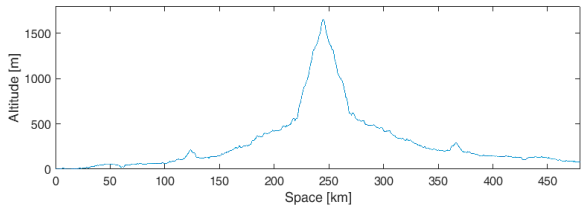

Figure 16. Highway + mountain mission altitude profile.

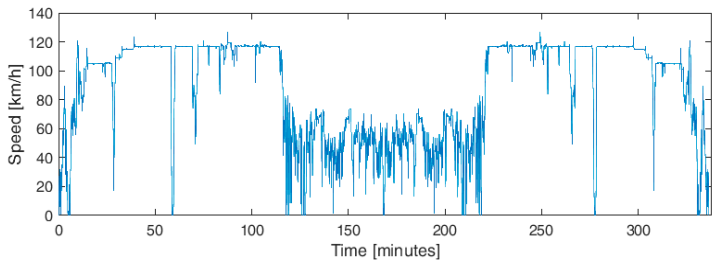

Figure 17. Highway + mountain mission speed profile.

5. Simulation Results

According to what previously shown in Section 3, NZ sizing is the first zone to be optimized. LSZ is a priori fixed to 30 Wh and braking zone to 100 Wh, indeed they do not have great influence on NZ sizing. Once NZ has been optimized, LSZ and BZ will be sized with the established NZ sizing. The monitored parameters, which are simulation outputs, vary stochastically on the same mission; as a matter of fact, ICE starts can occur at a certain moment depending on storage State Of Charge (SOC)

and, analogously, storable energy available during braking depends on storage SOC. For this reason, each road mission is repeated various times with different initial SOC. The output for that specific mission is considered as the averaged value over the different simulations.

5.1. Normal Zone Sizing

Normal zone aims at reducing ICE number of starts; according to EIMS shown in Figure 2, if speed is above USL, ICE turns on when SOC is at LVL, and turns off when UVL is reached. To establish if NZ is properly sized, one has to observe ICE starts when speed is above USL. As a matter of fact, ICE starts when speed is below USL depends on LSZ, and will be investigated in Section 5.2. Simulation results are shown in Table 3, where spark-ignition engine number of starts, while speed is above USL, is reported as a function of NZ sizing. Same results are reported in Table 4 for diesel engine. Indeed, been P_{min} different for spark-ignition engine and diesel engine, simulation results are different.

Table 3. Spark-ignition engine number of starts while speed is above Upper Speed Limit (USL) as a function of Normal Zone (NZ) sizing (i.e., NZ Wh). Values approximated to the nearest integer.

Missions	18 Wh	30 Wh	42 Wh	54 Wh	70 Wh	160 Wh
US06	6	5	4	4	4	4
UDDS	19	14	13	12	10	8
HWFET	5	4	3	3	2	1
Urban	26	17	12	11	11	10
Fast-urban	21	16	16	15	12	10
Extra-urban 1	35	26	18	14	11	5
Mountain mission 1	12	7	7	6	6	5
Extra-urban 2	39	35	30	28	21	11
Mountain mission 2	29	23	16	14	11	5
Highway + mountain	109	86	74	58	47	27

Table 4. Diesel engine number of starts while speed is above USL as a function of NZ sizing (i.e., NZ Wh). Values approximated to the nearest integer.

Missions	18 Wh	30 Wh	42 Wh	54 Wh	70 Wh	160 Wh
US06	7	7	6	5	4	3
UDDS	18	14	13	12	11	9
HWFET	5	4	3	2	2	1
Urban	21	20	18	14	14	10
Fast-urban	20	19	17	16	15	11
Extra-urban 1	29	20	16	12	10	4
Mountain mission 1	11	9	8	7	6	6
Extra-urban 2	34	31	27	27	21	9
Mountain mission 2	21	15	13	11	10	5
Highway + mountain	102	87	66	53	43	27

Since P_{min} is lower for diesel engine, the number of starts are lower in Table 4 for same NZ sizing. Indeed, diesel efficiency decrease slower for decreasing power demand compare to spark-ignition engine, as can be notice from Figure 1; as a consequence, storage system is charged slower in low-power missions and number of starts is reduced. Number of starts for NZ size of 18 Wh is very high and it decreases if zone sizing is increased. Nevertheless, moving from 70 Wh to 160 Wh, the number of starts slightly decrease; therefore, 70 Wh is considered the optimal compromise. In urban mission number of starts is anyway lower than a traditional vehicle with start and stop system. Moreover, Extra-urban 2 and Highway + Mountain missions are characterized by high number of ICE starts, but they are 55 min–57 km and 5.5 h–480 km, respectively; therefore, values in Table 4 are absolutely tolerable.

5.2. Low Speed Zone Sizing

Been NZ sizing fixed at 70 Wh, low speed zone sizing analysis was performed considering 70 Wh and 100 Wh for NZ and BZ, respectively. LSZ aim is to reduce number of ICE starts when speed is below USL; as a matter of fact one of hybrid vehicle objective is to perform electric traction at low speed. In Table 5, the ICE number of starts when speed is below USL are shown. While ICE ignitions when vehicle speed is above USL occurs normally and the NZ aim is just to limit them, ICE ignition when vehicle speed is below USL is an unwanted situation and therefore just very few of them are tolerable. One has to note that ICE starts when speed is below USL do not depend on P_{min}; therefore, Table 5 values concern both spark-ignition and diesel engines.

Table 5. Internal Combustion Engine (ICE) number of starts when speed is below USL, as a function of Low Speed Zone (LSZ) sizing (i.e., LSZ Wh).

Missions	10 Wh	15 Wh	20 Wh	30 Wh	50 Wh
US06	0	0	0	0	0
UDDS	0	0	0	0	0
HWFET	0	0	0	0	0
Urban	2	1.4	1.2	1	0.2
Fast-urban	4.2	3.2	3.2	2	1
Extra-urban 1	0	0	0	0	0
Mountain mission 1	0	0	0	0	0
Extra-urban 2	0	0	0	0	0
Mountain mission 2	3	3	2	2	0
Highway + mountain	1	0	0	0	0

As aforementioned, each mission was repeated several times in order to average simulation outputs; for this reason, decimal values are reported in Table 5.

One can observe that in standard type approvals, even a very small LSZ is sufficient not to have engine starts when speed is below USL. This aspect shows the need of introducing experimentally measured missions in order to evaluate powertrain behavior in real working conditions. As a matter of fact, values reported in Table 5 in 10 Wh sizing for urban missions (Urban and Fast-urban) and Mountain mission 2 are quite high. Low speed zone sizing at 30 Wh is considered sufficient to reduce ICE starts at a tolerable value.

5.3. Braking Zone Sizing

During the braking zone sizing study, NZ and LSZ sizing were fixed at 70 Wh and 30 Wh, respectively. BZ sizing directly influences powertrain efficiency, since backward energy has to be wasted on mechanical brakes once storage is fully charged. In Table 6 wasted energy on mechanical brakes as a percentage of energy provided by the generator is reported. Additionally, in this case, type approvals would not give enough information for a complete evaluation of storage sizing; indeed, energy waste is negligible already with 50 Wh BZ sizing. Moreover, in mission with long downhill roads (mountain mission 1, mountain mission 2 and highway + mountain), impact on fuel economy moving from 100 Wh to 270 Wh is not enough significant to justify such a great increase in BZ sizing. On balance, braking zone optimal sizing can be considered between 50 Wh and 100 Wh. As a matter of fact, this sizing is enough to recover all the backward energy in more than half of the proposed missions; in addition, in mountain missions, the benefit in terms of fuel consumption reduction, moving to a significantly higher BZ (e.g., 270 Wh), would be negligible. Fuel economy for spark-ignition engine is reported in Figure 18 and for diesel engine in Figure 19. One has to note that Table 6 data are the same for both type of ICE; indeed energy provided by the generator is the same in both cases, as well as wasted energy, while fuel economy is different been ICE efficiency different.

Table 6. Wasted energy on mechanical braking as a percentage of energy provided by generator, for various Braking Zone (BZ) sizing.

Missions	50 Wh	100 Wh	270 Wh
US06	3.7%	0	0
UDDS	0	0	0
HWFET	1%	0	0
Urban	0	0	0
Fast-urban	1.4%	0	0
Extra-urban 1	6%	4.7%	0
Mountain mission 1	28.6%	26.9%	19%
Extra-urban 2	0	0	0
Mountain mission 2	16.7%	16.5%	13%
Highway + mountain	3.7%	3.3%	3.0%

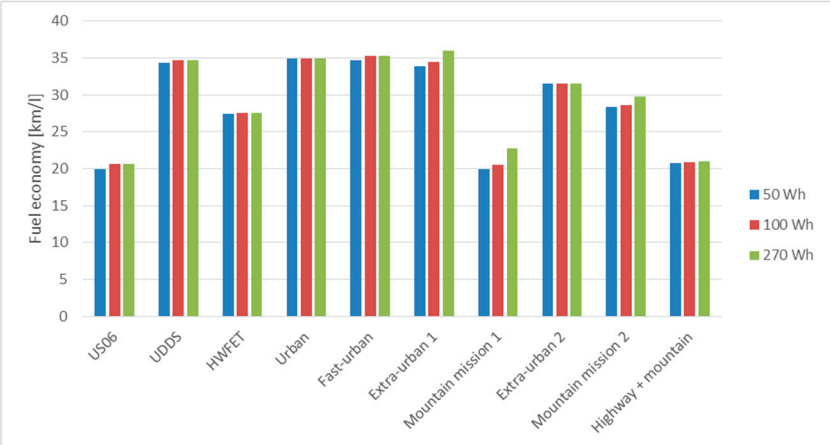

Figure 18. Fuel economy as a function of BZ sizing, spark-ignition engine.

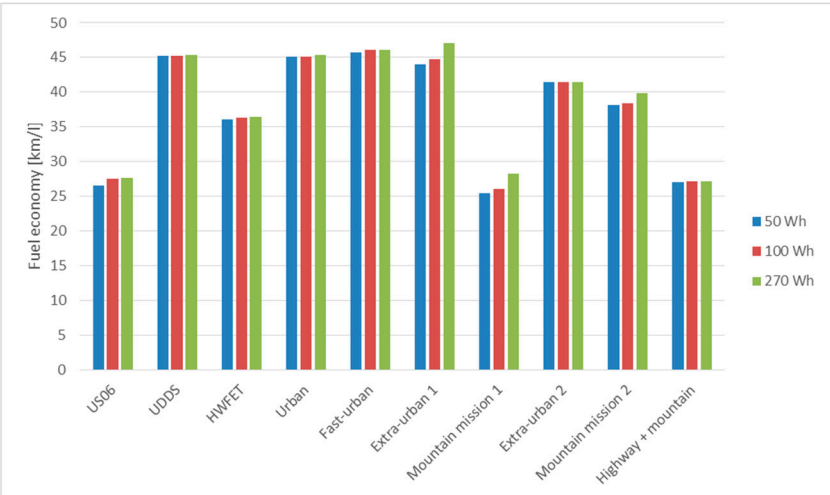

Figure 19. Fuel economy as a function of BZ sizing, diesel engine.

6. Conclusions

An analysis of supercapacitor storage sizing effect on hybrid series architecture was carried out in this study; a medium size car (i.e., 1450 kg) was considered. The impact both on ICE number of starts (which affects comfort) and on wasted energy on mechanical brakes (which influences powertrain efficiency) was taken into account. Simulation results demonstrated that standard type approvals do not properly model vehicle behavior; indeed, a storage sizing of about 100 Wh (e.g., 10 Wh for LSZ, 42

Wh for NZ and 50 Wh for BZ) would be enough to properly achieve all storage requirements. For this reason, seven experimentally measured missions were considered. Analyzing real working conditions, 150–200 Wh storage sizing is required (e.g., 30 Wh for LSZ, 70 Wh for NZ and 50–100 Wh for BZ). To recover all backward energy in mountain missions, storage sizing should be highly increased, becoming incompatible with vehicle applications. The proposed storage sizing (i.e., 150–200 Wh) is, instead, highly compatible with hybrid vehicle application, since it involves a storage weight of about 40–50 kg using EDLC supercapacitors, which can be further decreased to about 25–35 kg using lithium-ion supercapacitors.

Concluding, the increasing performance of supercapacitors has led to the possibility of realizing a series hybrid vehicle using only supercapacitors as storage system. The benefit of such types of architecture was shown in the technical literature and the feasibility, with regard to supercapacitor storage sizing, has been analyzed in detail in this paper. Moreover, the constantly increasing performance of such type of storage, together with the decreasing price, could further increase the interest for the proposed hybrid structure.

Author Contributions: M.P. conceived the article, developed the simulation model and wrote the article. S.G., S.W. and L.V. performed simulations and handled result diagrams. M.R. provided useful information on internal combustion engines and developed, together with M.P., the EMS. M.M. and M.C. supervised the all work and revised the article.

Funding: This research received no external funding.

Conflicts of Interest: The authors declare no conflict of interest.

References

1. Capata, R. Urban and extra-urban hybrid vehicles: A technological review. *Energies* **2018**, *11*, 2924. [CrossRef]
2. Salmasi, F.R. Control strategies for hybrid electric vehicles: Evolution, classification, comparison, and future trends. *IEEE Trans. Veh. Technol.* **2007**, *56*, 2393–2404. [CrossRef]
3. Uebel, S.; Murgovski, N.; Tempelhahn, C.; Bäker, B. Optimal energy management and velocity control of hybrid electric vehicles. *IEEE Trans. Veh. Technol.* **2017**, *67*, 327–337. [CrossRef]
4. Millo, F.; Cubito, C.; Rolando, L.; Pautasso, E.; Servetto, E. Design and development of an hybrid light commercial vehicle. *Energy* **2017**, *136*, 90–99. [CrossRef]
5. Chen, S.-Y.; Wu, C.-H.; Hung, Y.-H.; Chung, C.-T. Optimal strategies of energy management integrated with transmission control for a hybrid electric vehicle using dynamic particle swarm optimization. *Energy* **2018**, *160*, 154–170. [CrossRef]
6. Zhang, F.; Liu, H.; Hu, Y.; Xi, J. A supervisory control algorithm of hybrid electric vehicle based on adaptive equivalent consumption minimization strategy with fuzzy pi. *Energies* **2016**, *9*, 919. [CrossRef]
7. Hu, Y.; Li, W.; Xu, H.; Xu, G. An online learning control strategy for hybrid electric vehicle based on fuzzy q-learning. *Energies* **2015**, *8*, 11167–11168. [CrossRef]
8. Finesso, R.; Misul, D.; Spessa, E.; Venditti, M. Optimal design of power-split hevs based on total cost of ownership and co2 emission minimization. *Energies* **2018**, *11*, 1705. [CrossRef]
9. Burress, T.A.; Campbell, S.L.; Coomer, C.L.; Ayers, C.W.; Wereszczak, A.A.; Cunningham, J.P.; Marlino, L.D.; Seiber, L.E.; Lin, H.T. *Evaluation of the 2010 Toyota Prius Hybrid Synergy Drive System*; Power Electronics and Electric Machinery Research Facility, Technical Report ORNL/TM2010/253; Oak Ridge National Laboratory (ORNL): Oak Ridge, TN, USA, 2011.
10. Kim, N.; Cha, S.; Peng, H. Optimal control of hybrid electric vehicles based on pontryagin's minimum principle. *IEEE Trans. Control Syst. Technol.* **2011**, *19*, 1279–1287.
11. Bonfiglio, A.; Lanzarotto, D.; Marchesoni, M.; Passalacqua, M.; Procopio, R.; Repetto, M. Electrical-loss analysis of power-split hybrid electric vehicles. *Energies* **2017**, *10*, 2142. [CrossRef]
12. Cipek, M.; Pavković, D.; Petrić, J. A control-oriented simulation model of a power-split hybrid electric vehicle. *Appl. Energy* **2013**, *101*, 121–133. [CrossRef]
13. Pei, H.; Hu, X.; Yang, Y.; Tang, X.; Hou, C.; Cao, D. Configuration optimization for improving fuel efficiency of power split hybrid powertrains with a single planetary gear. *Appl. Energy* **2018**, *214*, 103–116. [CrossRef]

14. Xiang, C.; Ding, F.; Wang, W.; He, W. Energy management of a dual-mode power-split hybrid electric vehicle based on velocity prediction and nonlinear model predictive control. *Appl. Energy* **2017**, *189*, 640–653. [CrossRef]
15. Xu, Q.; Mao, Y.; Zhao, M.; Cui, S. A hybrid electric vehicle dynamic optimization energy management strategy based on a compound-structured permanent-magnet motor. *Energies* **2018**, *11*, 2212. [CrossRef]
16. Chen, J.; Du, J.; Wu, X. Fuel economy analysis of series hybrid electric bus with idling stop strategy. In Proceedings of the 2014 9th International Forum on Strategic Technology (IFOST), Cox's Bazar, Bangladesh, 21–23 October 2014; pp. 359–362.
17. Kim, M.; Jung, D.; Min, K. Hybrid thermostat strategy for enhancing fuel economy of series hybrid intracity bus. *IEEE Trans. Veh. Technol.* **2014**, *63*, 3569–3579. [CrossRef]
18. Zhao, Y.; Yao, J.; Zhong, Z.M.; Sun, Z.C. The research of powertrain for supercapacitor-based series hybrid bus. In Proceedings of the 2008 IEEE Vehicle Power and Propulsion Conference, Harbin, China, 3–5 September 2008; pp. 1–4.
19. Maxwell Supercapacitor. Available online: www.maxwell.com (accessed on 8 May 2019).
20. Ultimo Supercapacitor. Available online: https://www.jsrmicro.be/emerging-technologies/lithium-ion-capacitor/products/ultimo-lithium-ion-capacitor-laminate-cells-lic (accessed on 8 May 2019).
21. Cao, J.; Emadi, A. A new battery/ultracapacitor hybrid energy storage system for electric, hybrid, and plug-in hybrid electric vehicles. *IEEE Trans. Power Electron.* **2012**, *27*, 122–132.
22. Marchesoni, M.; Vacca, C. New DC–DC converter for energy storage system interfacing in fuel cell hybrid electric vehicles. *IEEE Trans. Power Electron.* **2007**, *22*, 301–308. [CrossRef]
23. Laldin, O.; Moshirvaziri, M.; Trescases, O. Predictive algorithm for optimizing power flow in hybrid ultracapacitor/battery storage systems for light electric vehicles. *IEEE Trans. Power Electron.* **2013**, *28*, 3882–3895. [CrossRef]
24. Marchesoni, M.; Savio, S. Reliability analysis of a fuel cell electric city car. In Proceedings of the 2005 European Conference on Power Electronics and Applications, Dresden, Germany, 11–14 September 2005; p. 10.
25. Carpaneto, M.; Ferrando, G.; Marchesoni, M.; Savio, S. A new conversion system for the interface of generating and storage devices in hybrid fuel-cell vehicles. In Proceedings of the IEEE International Symposium on Industrial Electronics, ISIE 2005, Dubrovnik, Croatia, 20–23 June 2005; pp. 1477–1482.
26. Kim, H.; Chen, H.; Zhu, J.; Maksimović, D.; Erickson, R. Impact of 1.2 kV SIC-MOSFET EV traction inverter on urban driving. In Proceedings of the 2016 IEEE 4th Workshop on Wide Bandgap Power Devices and Applications (WiPDA), Fayetteville, AR, USA, 7–9 November 2016; pp. 78–83.
27. Ding, X.; Cheng, J.; Chen, F. Impact of silicon carbide devices on the powertrain systems in electric vehicles. *Energies* **2017**, *10*, 533. [CrossRef]
28. Lanzarotto, D.; Marchesoni, M.; Passalacqua, M.; Prato, A.P.; Repetto, M. Overview of different hybrid vehicle architectures. *IFAC-PapersOnLine* **2018**, *51*, 218–222. [CrossRef]
29. Passalacqua, M.; Lanzarotto, D.; Repetto, M.; Vaccaro, L.; Bonfiglio, A.; Marchesoni, M. Fuel economy and energy management system for a series hybrid vehicle based on supercapacitor storage. *IEEE Trans. Power Electron.* **2019**. [CrossRef]
30. Zhang, L.; Hu, X.; Wang, Z.; Sun, F.; Deng, J.; Dorrell, D.G. Multiobjective optimal sizing of hybrid energy storage system for electric vehicles. *IEEE Trans. Veh. Technol.* **2018**, *67*, 1027–1035. [CrossRef]
31. Snoussi, J.; Elghali, S.B.; Benbouzid, M.; Mimouni, M.F. Optimal sizing of energy storage systems using frequency-separation-based energy management for fuel cell hybrid electric vehicles. *IEEE Trans. Veh. Technol.* **2018**, *67*, 9337–9346. [CrossRef]
32. Epa. Available online: https://www.epa.gov/vehicle-and-fuel-emissions-testing/dynamometer-drive-schedules (accessed on 8 May 2019).
33. Passalacqua, M.; Lanzarotto, D.; Repetto, M.; Marchesoni, M. Advantages of using supercapacitors and silicon carbide on hybrid vehicle series architecture. *Energies* **2017**, *10*, 920. [CrossRef]

34. Di Cairano, S.; Liang, W.; Kolmanovsky, I.V.; Kuang, M.L.; Phillips, A.M. Power smoothing energy management and its application to a series hybrid powertrain. *IEEE Trans. Control Syst. Technol.* **2013**, *21*, 2091–2103. [CrossRef]
35. Ortner, P.; Del Re, L. Predictive control of a diesel engine air path. *IEEE Trans. Control Syst. Technol.* **2007**, *15*, 449–456. [CrossRef]

© 2019 by the authors. Licensee MDPI, Basel, Switzerland. This article is an open access article distributed under the terms and conditions of the Creative Commons Attribution (CC BY) license (http://creativecommons.org/licenses/by/4.0/).